

Two Channel Description of Gas Permeability in Polymer-Grafted Nanoparticle Membranes

Arman Moussavi, William Marshall, Sanat K. Kumar,* and Sinan Keten*

Cite This: *Macromolecules* 2025, 58, 827–835

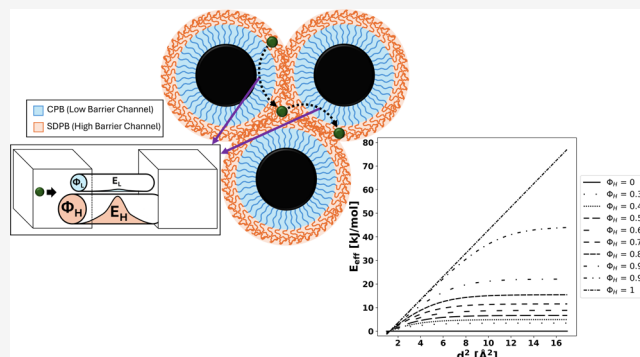
Read Online

ACCESS |

Metrics & More

Article Recommendations

ABSTRACT: Recent work has demonstrated that polymer-grafted nanoparticle (PGN) melts are spatially heterogeneous media with tunable gas transport properties. In particular, it is thought that the region near the nanoparticle (NP) surface, where the grafted chains are stretched due to crowding effects, as well as the interstitial regions within the NP packing, exhibit distinct transport behaviors. Based on these notions, this work proposes an analytical two channel model with a high-barrier channel akin to the pure polymer melt, and a low-barrier channel with zero activation energy. The model, developed with these simplifying assumptions, has one parameter, the fractional occupancy of the high-barrier channel, which is fit to gas permeability data as a function of chain molecular weight and gas type. Gases as big as CO₂ are present in both channels, while all larger gases primarily occupy the "high-barrier" channel. Since the model does not distinguish between solubility and diffusivity, it is concluded that the results found for the larger gases are consistent with the experimental findings showing that they have increased solubility within the interstitial spaces of the PGN structure. Similarly, the low channel corresponds to the stretched polymer brush with fast transport for all gases. Despite their higher fractional occupancy in the high-barrier channel, large gases also preferably transport through the low-barrier channel. The distinctions in energy barriers between the two channels manifest through a critical gas size beyond which the model's effective energy barrier becomes gas size-independent. This highlights the bilinear nature of gas transport in PGNs which results from their heterogeneous spatial structure.



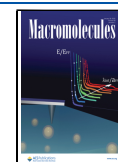
INTRODUCTION

Polymer membranes are widely used for separating gas mixtures due to their reduced energy cost compared to traditional separation methods, reliable mechanical stability under operational conditions, and ease of integration into existing industrial processes.^{1,2} Many industrial applications of polymer membranes rely on the size-selective permeability enabled by the polymer nanostructure.³ For instance, glassy polymers exhibit high selectivity in response to minor variations in penetrant size.³ This characteristic is advantageous in applications such as the separation of high-purity nitrogen from the air, the extraction of hydrogen from mixtures containing larger components, and the purification of natural gas.^{3,4} Often, membrane separation performance is characterized by the gas permeability and selectivity.⁵ Within the framework of the solution-diffusion model, the gas permeability, directly related to gas flux, is the product of the gas solubility and diffusion in the polymer. The selectivity of a membrane is determined by comparing the permeability coefficients of two gases, expressed as the ratio $\alpha_{A/B} = P_A/P_B$, where P_A and P_B denote the permeabilities of the more and less permeable gases, respectively.

The desired goal of designing polymer membranes with high permeability and high selectivity has prompted extensive research efforts. However, a well-established trade-off exists whereby polymers with higher permeability generally display less selectivity, and vice versa.^{5–8} Robeson notably characterized this relationship and its upper bound of the best available polymers for a given gas pair separation.^{5,6,9,10} While numerous methods have been investigated to improve the performance of traditional polymer membranes,^{11–13} polymer nanocomposites have emerged as promising membrane materials due to their novel polymer structures and superior separation properties.

In the context of gas separation, polymer-grafted nanoparticles (PGNs) are nanocomposite materials that have been shown to exhibit tunable transport properties. PGNs also

Received: October 29, 2024
Revised: December 11, 2024
Accepted: December 27, 2024
Published: January 10, 2025



possess enhanced mechanical properties, such as strength and durability, enabled by the superior dispersion effects resulting from grafting chains onto the nanoparticle surfaces.^{14–19} Moreover, chemically grafting the polymers onto the particles overcomes significant immiscibility challenges that typically hinder the formation of polymer nanocomposite membranes through the physical mixing of the constituents.^{20–23} Several studies in the literature have demonstrated that the permeability and separation performance of PGN membranes can be tuned by manipulating their structural parameters, such as NP size, grafted chain length, and grafting density, and free volume distribution.^{23–25} Bilchak et al. demonstrated that adding free polymer chains to the interstitial pockets between both rubbery PMA and glassy PMMA PGNs restricts the transport of larger gas molecules, thereby increasing gas selectivity with only a minor reduction in small gas permeability.²³ This finding suggests the presence of spatial heterogeneity within PGN membranes, characterized by regions with distinct polymer conformations and free volume distributions. While experimental work has suggested a rationale for the enhanced performance of PGN membranes, there lacks a theoretical framework to understand how spatial heterogeneities in the polymer nanocomposite structure influence size-based gas selectivity.

This work presents a model that attributes transport performance enhancements of PGNs to their heterogeneous structure, characterized by regions with unique polymer conformations and free volume distributions. The work of Bilchak et al.^{23–25} supplements this hypothesis by suggesting that the enhanced permeability arises from an increased diffusion coefficient, facilitated by distinct polymer conformations within regions where gas molecule transport occurs. This model integrates established theories of diffusion and permeability to explain the kinetics of the enhanced gas molecule transport through the heterogeneous nanostructure of PGNs. The model is demonstrated by fitting its parameters to data acquired from existing literature on gas transport through traditional linear polymer membranes. It is then applied to analyze permeability data for PGN membranes with the same chemical composition as those used in the fitting process. The model's key strength lies in its ability to isolate contributions to transport properties, such as permeability and activation energy barriers, that stem from the heterogeneous architecture of PGNs. It is generalizable as it can be adapted to model both glassy and rubbery polymers and be used to describe various heterogeneities idealized herein as phases with different transport and solubility characteristics (i.e., channels). Constants describing transport are in part taken to be universal across polymers based on experimental evidence, and polymer specific in others. In this study, for example, the permeability of PGN membranes with PMA grafts is predicted using permeability data from neat PMA. While the specified interpretations of this model to PGNs can be extended, for example to glassy PGNs, the specific constants for polymers such as PMMA would need to be obtained: such data do not exist at this time.

THEORY

The diffusion of gas molecules through polymeric media is postulated to be an activated process with an Arrhenius temperature dependence:

$$D = D_0 \cdot e^{-E_D/(R \cdot T)} \quad (1)$$

where D is the diffusion coefficient, D_0 is a pre-exponential factor, E_D is the activation energy required for diffusion through the medium, R is the gas constant, and T is the temperature. Bilchak et al. identified that the primary source of permeability enhancements in PGN membranes likely stems from an increase in the diffusion coefficient.²⁴ Consequently, the permeability of gas molecules through PGN membranes is expected to be captured by a similar Arrhenius temperature dependence as that described in eq 1. Equation 2 provides a rewritten formulation of the Arrhenius temperature dependence of permeability for the context of this study:

$$P = P_0 \cdot e^{-E_a/(R \cdot T)} \quad (2)$$

where P is the permeability and P_0 is a pre-exponential factor. Brandt demonstrated that the activation energy required for permeation (E_a) is related to the kinetic diameter (d) of a penetrating gas molecule:^{5,26}

$$E_a = c \cdot d^2 - f \quad (3)$$

where c and f are polymer-dependent constants, which can be determined by fitting eq 3 with neat polymer melt data. These quantities are extensively reported throughout the published literature. Typically, large values of c and f correspond to high diffusivity selectivity and stiffer polymers, respectively.^{5,27} In this study, the polymer constants c and f , derived from the fitting procedure, are directly applied to PGN membranes possessing identical grafted polymer chain chemistry as the neat polymer melt used in the fitting of eq 3. A relationship describing P_0 of eq 2 has been previously identified by Barrer and Amerongen.^{28,29} This “linear free energy” relationship is rationalized by an enthalpy–entropy compensation effect³⁰ and is herein modified for permeability in eq 4:

$$\ln[P_0] = a \cdot \frac{E_a}{R} - b \quad (4)$$

where a and b are constants. For diffusion through pure polymers, the first term of the linear free energy relationship typically appears as $a_D \cdot \frac{E_D}{R \cdot T}$, where a_D has been demonstrated to be independent of polymer type.³⁰ Additionally, throughout the literature, larger values of b_D correspond to stiffer polymers.³¹ In this study, eq 4 is fitted using permeability data of neat polymer melts to determine the constants a and b , where a holds the unit of Kelvin⁻¹ to ensure unit consistency.

TWO CHANNEL MODEL

The structural attributes of PGNs such as grafted polymer molecular weight, grafting density, and nanoparticle surface curvature have been extensively shown to correlate with the formation of polymer brushes.^{14,32–36} At moderate-to-high grafting densities polymer chains assume concentrated polymer brush (CPB) conformations due to confinement effects near the nanoparticle surface. Surface curvature and neighboring grafted chain restrictions facilitate highly stretched and well ordered polymer chain segments in this region. Further away from the nanoparticle surface, polymer chains assume a semidilute polymer brush (SDPB) conformation. In this region, the segments of the grafted chains assume their Gaussian conformations reminiscent of the melt state.^{32,34–39} The extent of each region is characterized by the “concentrated polymer brush to semidilute polymer brush” (CPB-SDPB) transition that has been well studied in PGN systems.^{34,36,40}

Previous experimental studies on the permeability of both rubbery PMA and glassy PMMA neat PGN membranes have demonstrated that adding free polymer chains to the membrane can enhance gas selectivity.²³ Long free polymer chains added to the neat PGN membrane reside in interstitial pockets between the NPs, while shorter free chains disperse throughout the grafted chains. It is hypothesized that the interstitial regions provide larger free volume pockets, which are more accommodating for free chains comparable in length to the grafts. The addition of long chains inhibits the transport of large gases, resulting in large increases in selectivity. These results suggest that large gas molecules are likely solubilized within the interstitial regions of PGN membranes. The transport of smaller gases, for example, CO₂, is found to be independent of the addition of free polymer chains, suggesting that small gases likely solubilize throughout the entire membrane.

The fundamental premise of the model devised to capture these attributes is that the heterogeneous structure of a composite membrane can be idealized as two channels characterized by distinctly different permeability. This work hypothesizes that these channels correspond to the CPB and SDPB regions, each holding a distinct energy barrier. Recent experimental work demonstrated that the activation energy (E_a) of PGN melts derived from the temperature dependence of relaxation times displays a pronounced minimum at intermediate grafted chain molecular weights (50–75 [kDa] for poly(methyl acrylate) PMA at a grafting density of ≈ 0.47 [chains/nm²]).²⁵ This finding is rationalized by the theoretically established notion that these chains exhibit the highest degree of extension based on a geometric crossover within the two-layer model of PGN structures proposed by Midya et al.³² This crossover appears to correlate with a minimum in the normalized monomer friction coefficients, which contributes to the observed decrease in activation energy. Similar reductions in monomeric friction were observed by Bobbili and Milner through simulations of stretched polymer melts in both flexible and stiff polymer systems.⁴¹ As a consequence of the activation energy minimum accompanied by a decreased monomeric friction coefficient for extended chain conformations, the CPB region of PGN membranes is expected to yield locally accelerated dynamics, leading to increased permeabilities.⁴²

Based on this rationale, a two channel model for gas transport in PGNs is proposed. The first channel, representing the SDPB region, is postulated to behave akin to an ungrafted linear polymer membrane. This channel is designated as the high-barrier channel (HBC). By analogy with transport in a linear polymer, it is proposed that the permeability of a gas molecule through the HBC follows:

$$P_H = P_{OH} \cdot e^{-E_H/(R \cdot T)} \equiv P_{OH} \cdot e^{(-c \cdot d^2 + f)/(R \cdot T)} \quad (5)$$

where P_{OH} is the pre-exponential factor of the HBC and E_H is the energy barrier required for permeation through the HBC. $\ln[P_{OH}]$ is described by the linear free energy relation observed by Barrer and Amerongen (eq 6):

$$\ln[P_{OH}] = a \cdot \frac{E_H}{R} - b \quad (6)$$

where a relationship with the high energy barrier is employed. Combining these variables in the construction of eq 5 allows for modeling permeability through the HBC.

The second transport pathway, the low-barrier channel (LBC), represents the CPB region and is associated with a reduced energy barrier.²⁵ It is proposed that $E_L = k \cdot E_H$, where k is a small constant assumed here to be 0 to signify a barrierless channel for transport. This assumption is motivated by the desire to explore the theoretical extreme case of no energy barrier to transport through the channel, providing an idealized baseline for the two channel model. The permeability of a gas molecule through the LBC thus follows $P_L = P_{OL}$ where P_{OL} is the pre-exponential factor of the LBC which follows the linear free energy relation observed by Barrer and Amerongen $\ln[P_{OL}] = -b$.

The total permeability through PGN membranes with this model combines the permeability of the HBC and LBC into an effective permeability. This is done by using a fractional contribution written by eq 7:

$$P_{\text{eff}} = \Phi_L \cdot P_{OL} + \Phi_H \cdot P_{OH} \cdot e^{-E_H/(R \cdot T)} \\ = e^{-b} [\Phi_L + \Phi_H e^{a \cdot E_H/R} e^{(-c \cdot d^2 + f)/(R \cdot T)}] \quad (7)$$

where Φ_L and Φ_H are introduced terms that denote the fractional occupancy of the LBC and the HBC, respectively. $\Phi_L + \Phi_H = 1$. The fractional occupancy terms are regarded as the solubility of gas molecules in each region of the PGN membrane and are fitted to empirical data to complete the two channel permeability model. The parameters c , f , a , and b , derived from the homogeneous membrane, are directly applied to the grafted nanoparticle system, as they are solely used for the HBC with relaxed polymer conformations, where diffusion characteristics are comparable to the neat polymer melt.

RESULTS AND DISCUSSION

To showcase the application of the derived model, specific gas molecule permeability data through neat polymer membranes from prior literature is first analyzed to fit the constants c , f , a , and b for the activation energy and pre-exponential terms. Temperature dependent permeability for the transport of noble gases through a neat PMA membrane with the molecular weight of 4.6×10^6 [g/mole] is extracted from previous work by Burgess et al.⁴³ using a plot-digitizer data-point extraction tool.⁴⁴ The data acquired spans the gases of He, Ne, Ar, and Kr, with kinetic diameters of ≈ 2.6 , 2.75, 3.4, and 3.6 [Å], respectively. The Arrhenius plots of neat PMA permeability to noble gases originating from Burgess et al. are recreated for clarity and reference in Figure 1.

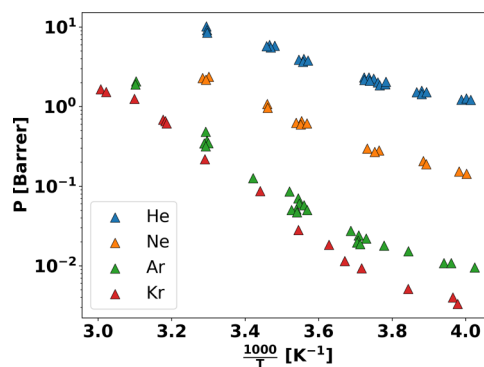


Figure 1. Temperature-dependent permeability of noble gases through neat PMA membranes. Redrawn from ref 43, copyright 1971 Marcel Dekker, Inc.

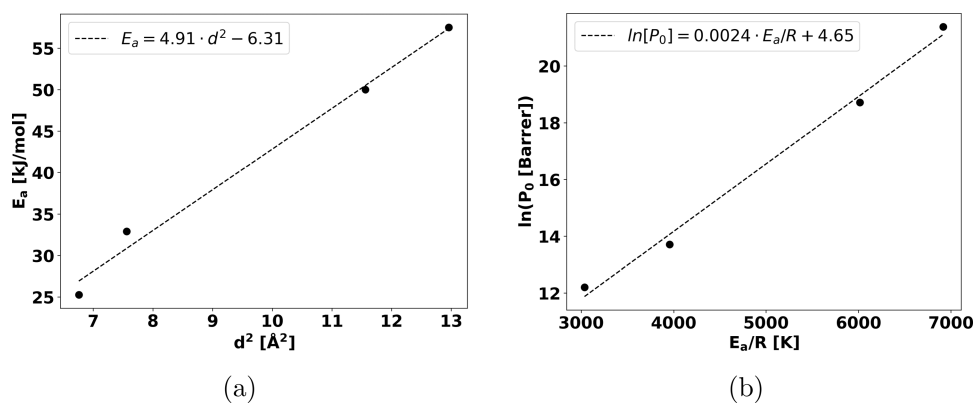


Figure 2. (a) Polymer constants c and f derived using eq 3. (b) Polymer constants a and b derived using eq 4.

First, high temperature data (above the glass transition temperature of PMA) is fitted to obtain the P_0 and E_a for a homopolymer membrane model (single channel) for each gas. In Figure 4a, eq 3 has been fitted to the data extracted from Burgess et al. From the fit, the polymer constants are determined to be $c = 4.91$ [kJ/(mol \cdot \AA^2)] and $f = 6.31$ [kJ/mol]. The constants a and b of eq 4 are evaluated utilizing the same data set. Figure 4b illustrates the fit of eq 4 to the data set. The constants are found to be $a = 0.0024$ [K^{-1}] and $b = -4.65$. Fitting the constants c , f , a , and b in both the activation energy and pre-exponential terms facilitates fitting the PGN data using the two channel model (Figure 2).

The HBC and LBC fractional occupancy terms (Φ_H and Φ_L) of the effective permeability are unknown through the derivation of the two channel model. The temperature-dependent permeability of gas molecules (with a specified kinetic diameter) transporting through a PGN membrane is used to determine Φ_H as a function of gas size, PGN chain molecular weight, and temperature. To demonstrate this procedure, the focus is placed on data for different gases at a single temperature of 308.15 [K]^{23,24} (Figure 3). Figure 4a

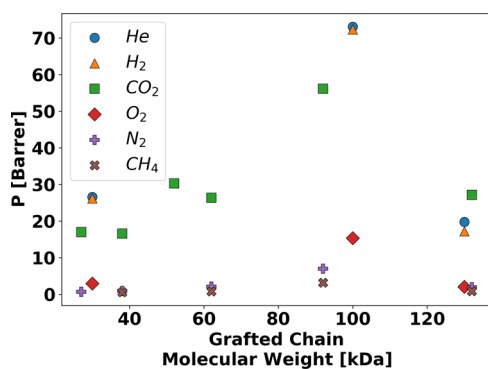


Figure 3. Permeability of several gases through PMA grafted nanoparticle membranes. Redrawn from ref 23, copyright 2020 American Chemical Society and ref 24, copyright 2017 American Chemical Society.

provides the determined Φ_H as a function of the molecular weight of the grafted PMA chains for the available data. Table 1 has been added to display the individual values of each point.

Figure 4a illustrates several important points. First, a clear change in behavior is observed when transitioning from small gases (H_2 , He and CO_2) to large gases (O_2 , N_2 and CH_4). Larger gases exhibit larger Φ_H values. This is consistent with

the experimental suggestions that large gases solubilize in the SDPB region of PGN membranes.²³ Furthermore, the transition in behavior occurs for gases larger than CO_2 , again in good agreement with experiments. Another observation is that the Φ_H values go through a minimum in the vicinity of the highest gas permeability region, ≈ 100 [kDa]. These results suggest that the small gases tend to diffuse preferentially through the low-barrier channel, a trend that becomes accentuated in regions where the polymer chains are most extended, as highlighted by the minimum in Φ_H . This behavior can be explained by the observation made by Jhalaria et al., which shows that the maximum degree of chain stretching and a minimum in the calculated activation energy are correlated, both occurring at an intermediate grafted chain length.²⁵ This intermediate chain length accompanies the transition from a dry layer-dominated regime to an interpenetrated layer-dominated regime.³² The observed nonmonotonic behavior of Φ_H aligns with this transition point, suggesting that all gases achieve their maximum solubility within the LBC, corresponding to the minimum of Φ_H . As discussed further below, this observation justifies the proposal that the low-barrier channel corresponds to the stretched polymer brush. Consequently, the high-barrier channel likely represents the interstitial spaces within the PGN assembly, which exhibit behavior analogous to that of a polymer melt.

Examining the individual permeability contributions of each channel offers greater insight into the relative role of the two channels in gas transport. To accomplish this, $\Psi = \frac{\Phi_L \cdot P_{0L}}{P_{eff}}$ is defined as the fractional contribution of the LBC to gas permeability. Ψ is plotted as a function of grafted polymer molecular weight in Figure 4b and tabulated in Table 2. The small gases (He, H_2 , and CO_2) are primarily transported through the LBC. This is an expected result based on the concept illustrated in Figure 4a. Analysis of Ψ for large gases reveals the underlying significance of this model. Large gases (O_2 , N_2 , and CH_4) generally display large values of Ψ . Although this result appears to contrast the observations presented in Figure 4a, it indeed follows the theoretical expectation of this model. That is, large gases primarily utilize the LBC for transport. Despite large gases having access to only a small fraction of the LBC, they demonstrate a significantly higher inclination to utilize the low-barrier pathway when the opportunity arises. This phenomenon is depicted by Figure 4b, where large gases tend to traverse the LBC even when Φ_L is small. Another pertinent observation regarding these results is the marginal increase in Ψ at 92

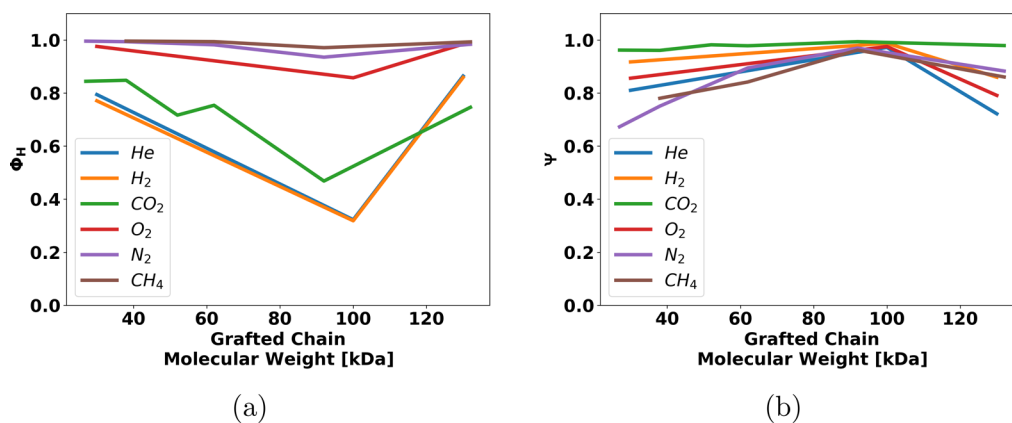


Figure 4. (a) Fractional occupancy of the HBC, and (b) contribution of the LBC's permeability to the effective PGN membrane permeability, as a function of grafted PMA chain molecular weight.

Table 1. Φ_H Solution for Gas and Grafted Polymer Chain Molecular Weight

gas	polymer MW								
	27 kDa	30 kDa	38 kDa	52 kDa	62 kDa	92 kDa	100 kDa	130 kDa	132 kDa
He		0.794					0.323	0.864	
H ₂		0.771					0.319	0.859	
CO ₂	0.844		0.848	0.717	0.754	0.468			0.746
O ₂		0.976					0.857	0.984	
N ₂	0.996		0.994		0.982	0.935			0.984
CH ₄			0.996		0.994	0.971			0.993

Table 2. Ψ Solution for Gas and Grafted Polymer Chain Molecular Weight

gas	polymer MW								
	27 kDa	30 kDa	38 kDa	52 kDa	62 kDa	92 kDa	100 kDa	130 kDa	132 kDa
He		0.810					0.972	0.722	
H ₂		0.917					0.988	0.860	
CO ₂	0.962		0.961	0.982	0.978	0.993			0.979
O ₂		0.856					0.975	0.791	
N ₂	0.673		0.751		0.895	0.969			0.883
CH ₄			0.780		0.842	0.962			0.861

[kDa] correlating to a significantly amplified effect on the contribution of the LBC to the total permeability.

The findings suggest that there must be a change in transport behavior with increasing gas size in which larger gas molecules transporting through the membrane depict a lower Φ_L . To further understand these results, a range of Φ_H values is selected, and for each value, P_{eff} is calculated as a function of gas size using the two channel model. Writing $P_{\text{eff}} = P_{0\text{eff}} \cdot \exp\left[\frac{-E_{\text{eff}}}{R \cdot T}\right]$, the effective activation energy barrier (E_{eff}) is solved as a function of the kinetic gas diameter squared (d^2) (Figure 5).

Figure 5 portrays the expected transition in activation energy as a function of the gas diameter squared. For small gases, E_{eff} follows the behavior of transport through a linear polymer membrane. More importantly, once a critical gas size is exceeded and extends to larger gas molecules, E_{eff} plateaus. The gas size independence of the energy barrier to transport is based on the observation that small gas molecules tend to solubilize uniformly across the entire membrane, yet preferentially permeate through the LBC due to its reduced energy barrier. In contrast, larger gas molecules, while also capable of solubilizing within the HBC, strongly favor

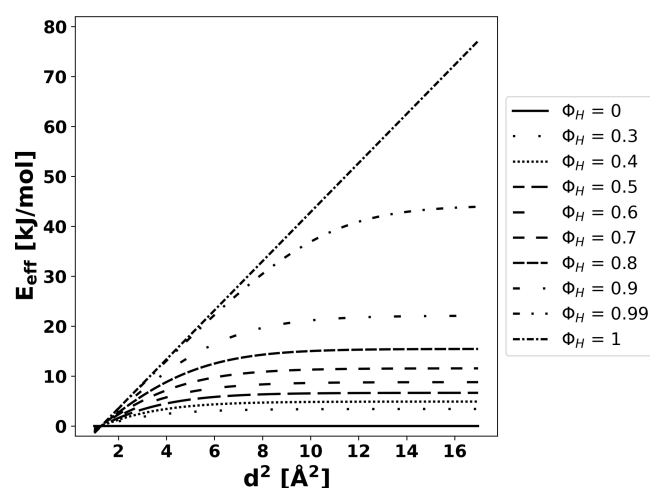


Figure 5. E_{eff} solution of a range of values for Φ_H .

transport through the LBC. This preference arises as the energy barrier within the HBC increases quadratically with gas size, making it energetically unfavorable for larger gases to permeate through this region. Consequently, larger gas

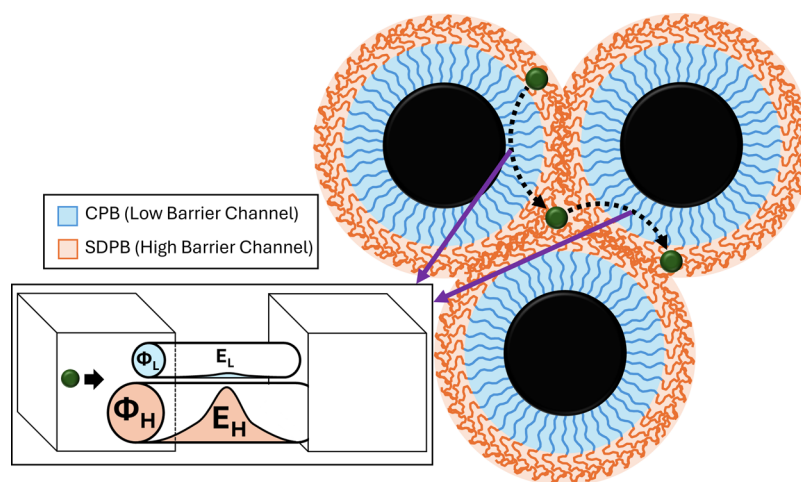


Figure 6. Schematic illustration of gas transport through the two channel model.

molecules are driven to diffuse through the LBC, where the lower energy barrier and higher permeability facilitate their transport. As a result, the overall transport process is dominated by the permeability of the LBC.

The two channel model is schematically illustrated in Figure 6. The large black circles represent nanoparticles. The polymer chains grafted onto the surface of the nanoparticles are split into two regions, the CPB and SDPB which correspond to the LBC and HBC, respectively. A gas molecule is depicted in green, at three stages of permeation.

The physical interpretation of this model is as follows: A gas molecule permeating through a PGN membrane solubilizes mainly within the HBC. Here, this molecule encounters two parallel pathways: the HBC and LBC. Due to the significantly lower energy barrier in the LBC, gas molecules primarily diffuse through this channel to reach another highly probable HBC region (where solubility is high).

To further explore how this model can be applied to a broader range of PGN systems, particularly those with varying polymer stiffness, the polymer-dependent constants were varied. This study was performed given the limited availability of experimental data for other PGN membranes in the literature. The three sets of constants were selected with even spacing, based on typical polymer values proposed by Freeman.⁵ The parameter a , derived from the permeability of PMA, was held constant across all models, consistent with Freeman's assertion that a is independent of polymer type. The parameter range for b was chosen between 9.2 and 11.5 since Freeman suggested 9.2 for rubbery polymers and 11.5 for glassy polymers. The values of c and f derived for neat PMA fall in Freeman's suggested range. A range of 1.046 (for extremely flexible polymers) to 10.0416 (for stiff-chain, glassy polymers) [kJ/(mol · Å²)] is selected for c , and 0 (for rubbery polymers) to 58.576 (for glassy polymers) [kJ/(mol)] for f . The chosen constants for each system are provided in Table 3.

Table 3. Variation of Polymer-Dependent Constants c , f , and b

polymer	c [kJ/(mol · Å ²)]	f [kJ/(mol)]	b
flexible, rubbery	1.046	0.000	9.200
moderately stiff	5.544	29.288	10.350
very stiff, glassy	10.042	58.576	11.500

The low activation energy of the rubbery system's HBC relative to glassy systems leads to a smooth and gradual transition at the critical gas size, Figure 7a. The final plateau in E_{eff} is reached only at larger values of d^2 . In the moderately stiff polymer system (Figure 7b), the higher activation energy of the HBC results in a more pronounced transition at the critical gas size, with the plateau in E_{eff} being reached at a smaller value of d^2 . Finally, the very stiff, glassy system, as shown in Figure 7c, exhibits a sharp transition at a specific gas size, shifting from HBC-dominated to LBC-dominated permeation. In this case, the plateau in E_{eff} is reached almost immediately. This behavior indicates that very stiff polymers impose significant restrictions on permeation through the HBC. Beyond the critical gas size, molecules are driven through the LBC due to extremely high activation energy penalties. Brandt's model of activation energy provides a strong theoretical foundation, showing that stiffer polymers inherently exhibit larger activation energy barriers, which directly aligns with the trends observed in Figure 7. Furthermore, the bilinear nature of E_{eff} for gas transport through PGNs, as predicted by this model, is validated by the findings of Jhalaria et al., who demonstrated a clear correlation between chain extension and reduced activation energy, suggesting locally accelerated dynamics in the CPB region of PGN membranes. These correlations provide compelling evidence that the model accurately captures the key transport mechanisms, particularly the gas size-dependent transition from HBC to LBC-dominated permeation, and is well-suited to describe permeability behavior across a wide range of PGN materials. Moreover, this demonstrates the generalizability of the model findings and how key parameters can be used to tailor membrane behavior to augment conventional size-scaling laws for transport via heterogeneity.

CONCLUSIONS

This work provides a simple analytical theoretical framework aimed at understanding the underlying mechanisms of gas molecule transport through a heterogeneous material, with a specific focus on polymer-grafted nanoparticle (PGN) membranes. The model defines two transport channels within the heterogeneous structure of a PGN melt. The first channel corresponds to the semidilute polymer brush (SDPB), which resembles the properties of a neat polymer melt and is referred to as the high-barrier channel (HBC). The second channel corresponds to the concentrated polymer brush (CPB) region,

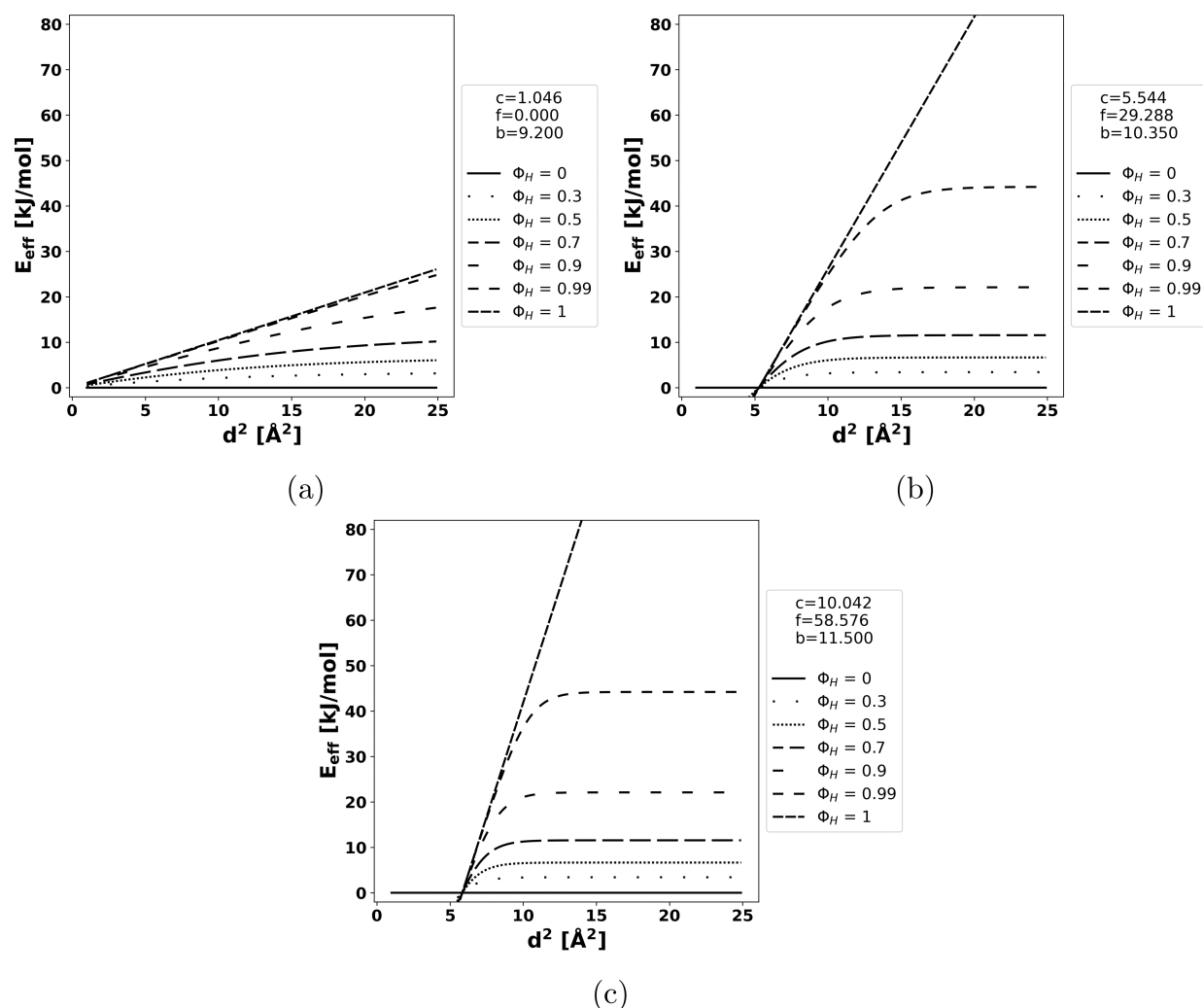


Figure 7. (a) Model of a flexible, rubbery polymer (b) moderately stiff polymer (c) very stiff, glassy polymer.

which significantly accelerates transport dynamics. This acceleration is due to a lowered effective activation energy barrier resulting from a reduction in local monomeric friction. Consequently, this is referred to as the low-barrier channel (LBC). By defining these distinct phases within the structure of a PGN membrane, the model characterizes the gas molecule size-dependent transport. Leveraging simplistic parametrization from conventional linear polymer membranes, the permeability data of PGN membranes extracted from the literature serves as a basis for predicting size-dependent transport mechanisms. Large gas molecules are predicted to predominantly solubilize within the phase holding characteristics akin to neat polymer melts. Small gases exhibit inherent ability to solubilize throughout the melt-like and accelerated dynamics phases. According to these predictions, the LBC contribution to the effective permeability suggests that both small and large gases prefer transport through the LBC. This preference is a consequence of the significantly reduced energy barrier necessary to overcome for permeation. The effective activation energy barrier derived from the model reinforces the results of transport preference by revealing the underlying bilinear nature of the two channel model. Gas molecules transport indiscriminately throughout the entire membrane up to a critical size, however, once this critical size is exceeded, gases preferentially utilize the channel with the reduced barrier.

Finally, an illustration is provided to interpret the mechanisms of transport through PGN membranes proposed by this model. By bridging the gap between experimental insights and a novel theoretical basis, this model contributes to refining the current understanding of gas transport phenomena through heterogeneous materials, particularly PGN membranes. This work also demonstrates that the underlying structure of this model can be extended to a variety of material systems, provided that the model parameters are carefully adjusted to account for the specific properties of each system. While the assumptions and interpretations in this work were developed specifically for PGNs, future research should explore their applicability to other heterogeneous membrane materials. The model proposed here offers a versatile framework for describing transport phenomena across various membrane systems, where factors like polymer conformation and energy barriers may differ. Its transferability lies in its ability to capture the influence of heterogeneity, rather than being constrained by specific factors like polymer chemistry, which would otherwise limit its use to PGNs. In principle, the model is also generalizable to other systems with heterogeneous transport properties that can be interpreted as consisting of two phases, such as membranes with local inhomogeneities or defects. Expanding the understanding of gas transport dependencies on factors such as membrane chemistry and polymer structure will

enable a more comprehensive characterization of gas transport within emerging material systems. This, in turn, will facilitate the development of tunable membranes that optimize future gas separation technologies.

AUTHOR INFORMATION

Corresponding Authors

Sanat K. Kumar – Department of Chemical Engineering, Columbia University, New York, New York 10027, United States; orcid.org/0000-0002-6690-2221; Email: sk2794@columbia.edu

Sinan Ketten – Department of Civil and Environmental Engineering and Department of Mechanical Engineering, Northwestern University, Evanston, Illinois 60208, United States; orcid.org/0000-0003-2203-1425; Email: s-ketten@northwestern.edu

Authors

Arman Moussavi – Department of Civil and Environmental Engineering, Northwestern University, Evanston, Illinois 60208, United States

William Marshall – Department of Chemical Engineering, Columbia University, New York, New York 10027, United States

Complete contact information is available at:

<https://pubs.acs.org/10.1021/acs.macromol.4c02541>

Notes

The authors declare no competing financial interest.

ACKNOWLEDGMENTS

Authors acknowledge funding from the National Science Foundation (award number DMR-2226081).

REFERENCES

- (1) Robeson, L. Polymer membranes for gas separation. *Curr. Opin. Solid State Mater. Sci.* **1999**, *4*, 549–552.
- (2) Lasseguette, E.; Comesaña-Gándara, B. Polymer membranes for gas separation. *Membranes* **2022**, *12*, 207.
- (3) Freeman, B.; Pinnau, I. *Polymeric materials for gas separations*; ACS Publications, 1999; pp 1–27.
- (4) Paul, D. R. *Polymeric gas separation membranes*; CRC press, 2018; pp 513–614.
- (5) Freeman, B. D. Basis of permeability/selectivity tradeoff relations in polymeric gas separation membranes. *Macromolecules* **1999**, *32*, 375–380.
- (6) Robeson, L. M. Correlation of separation factor versus permeability for polymeric membranes. *Journal of membrane science* **1991**, *62*, 165–185.
- (7) Stern, S. A. Polymers for gas separations: the next decade. *J. Membr. Sci.* **1994**, *94*, 1–65.
- (8) Robeson, L.; Burgoyne, W.; Langsam, M.; Savoca, A.; Tien, C. High performance polymers for membrane separation. *Polymer* **1994**, *35*, 4970–4978.
- (9) Robeson, L. M. The upper bound revisited. *Journal of membrane science* **2008**, *320*, 390–400.
- (10) Sanders, D. F.; Smith, Z. P.; Guo, R.; Robeson, L. M.; McGrath, J. E.; Paul, D. R.; Freeman, B. D. Energy-efficient polymeric gas separation membranes for a sustainable future: A review. *Polymer* **2013**, *54*, 4729–4761.
- (11) Hachisuka, H.; Ohara, T.; Ikeda, K.-I.; Matsumoto, K. Gas permeation property of polyaniline films. *J. Appl. Polym. Sci.* **1995**, *56*, 1479–1485.
- (12) Park, H. B.; Jung, C. H.; Lee, Y. M.; Hill, A. J.; Pas, S. J.; Mudie, S. T.; Van Wagner, E.; Freeman, B. D.; Cookson, D. J. Polymers with cavities tuned for fast selective transport of small molecules and ions. *Science* **2007**, *318*, 254–258.
- (13) McKeown, N. B.; Budd, P. M. Polymers of intrinsic microporosity (PIMs): organic materials for membrane separations, heterogeneous catalysis and hydrogen storage. *Chem. Soc. Rev.* **2006**, *35*, 675–683.
- (14) Hore, M. J.; Korley, L. T.; Kumar, S. K. Polymer-grafted nanoparticles. *J. Appl. Phys.* **2020**, *128*, No. 030401.
- (15) Kumar, S. K.; Benicewicz, B. C.; Vaia, R. A.; Winey, K. I. 50th anniversary perspective: Are polymer nanocomposites practical for applications? *Macromolecules* **2017**, *50*, 714–731.
- (16) Kumar, S. K.; Jouault, N.; Benicewicz, B.; Neely, T. Nanocomposites with polymer grafted nanoparticles. *Macromolecules* **2013**, *46*, 3199–3214.
- (17) Kumar, S. K.; Krishnamoorti, R. Nanocomposites: structure, phase behavior, and properties. *Annu. Rev. Chem. Biomol. Eng.* **2010**, *1*, 37–58.
- (18) Balazs, A. C.; Emrick, T.; Russell, T. P. Nanoparticle polymer composites: where two small worlds meet. *Science* **2006**, *314*, 1107–1110.
- (19) Moussavi, A.; Pal, S.; Wu, Z.; Ketten, S. Characterizing the shear response of polymer-grafted nanoparticles. *J. Chem. Phys.* **2024**, *160*, 134903.
- (20) Merkel, T.; Freeman, B.; Spontak, R.; He, Z.; Pinnau, I.; Meakin, P.; Hill, A. Ultraporous, reverse-selective nanocomposite membranes. *Science* **2002**, *296*, 519–522.
- (21) Galizia, M.; Chi, W. S.; Smith, Z. P.; Merkel, T. C.; Baker, R. W.; Freeman, B. D. 50th anniversary perspective: polymers and mixed matrix membranes for gas and vapor separation: a review and prospective opportunities. *Macromolecules* **2017**, *50*, 7809–7843.
- (22) Takahashi, S.; Paul, D. Gas permeation in poly (ether imide) nanocomposite membranes based on surface-treated silica. Part 1: Without chemical coupling to matrix. *Polymer* **2006**, *47*, 7519–7534.
- (23) Bilchak, C. R.; Jhalaria, M.; Huang, Y.; Abbas, Z.; Midya, J.; Benedetti, F. M.; Parisi, D.; Egger, W.; Dickmann, M.; Minelli, M.; et al. Tuning selectivities in gas separation membranes based on polymer-grafted nanoparticles. *ACS Nano* **2020**, *14*, 17174–17183.
- (24) Bilchak, C. R.; Buenning, E.; Asai, M.; Zhang, K.; Durning, C. J.; Kumar, S. K.; Huang, Y.; Benicewicz, B. C.; Gidley, D. W.; Cheng, S.; et al. Polymer-grafted nanoparticle membranes with controllable free volume. *Macromolecules* **2017**, *50*, 7111–7120.
- (25) Jhalaria, M.; Huang, Y.; Ruzicka, E.; Tyagi, M.; Zorn, R.; Zamponi, M.; García Sakai, V.; Benicewicz, B.; Kumar, S. Activated transport in polymer grafted nanoparticle melts. *Macromolecules* **2021**, *54*, 6968–6974.
- (26) Brandt, W. W. Model calculation of the temperature dependence of small molecule diffusion in high polymers. *J. Phys. Chem.* **1959**, *63*, 1080–1085.
- (27) HARAYA, K.; OBATA, K.; HAKUTA, T.; YOSHITOME, H. The Permeation of Gases through a New Type Polyimide Membrane. *membrane* **1986**, *11*, 48–52.
- (28) Barrer, R. M. Permeability in relation to viscosity and structure of rubber. *Rubber Chem. Technol.* **1942**, *15*, 537–544.
- (29) Van Amerongen, G. J. The permeability of different rubbers to gases and its relation to diffusivity and solubility. *J. Appl. Phys.* **1946**, *17*, 972–985.
- (30) Barrer, R.; Skirrow, G. Transport and equilibrium phenomena in gas–elastomer systems. I. Kinetic phenomena. *J. Polym. Sci.* **1948**, *3*, 549–563.
- (31) Van, D. *Properties of Polymers, their Correlation with Chemical Structure; their Numerical Estimation and Prediction from Additive Group Contributions*; Rev. 2nd Impression; ELSEVIER, 1990.
- (32) Midya, J.; Rubinstein, M.; Kumar, S. K.; Nikoubashman, A. Structure of Polymer-Grafted Nanoparticle Melts. *ACS Nano* **2020**, *14*, 15505–15516.
- (33) Rungta, A.; Natarajan, B.; Neely, T.; Dukes, D.; Schadler, L. S.; Benicewicz, B. C. Grafting bimodal polymer brushes on nanoparticles using controlled radical polymerization. *Macromolecules* **2012**, *45*, 9303–9311.

(34) Dukes, D.; Li, Y.; Lewis, S.; Benicewicz, B.; Schadler, L.; Kumar, S. K. Conformational transitions of spherical polymer brushes: synthesis, characterization, and theory. *Macromolecules* **2010**, *43*, 1564–1570.

(35) Li, T.-H.; Yadav, V.; Conrad, J. C.; Robertson, M. L. Effect of Dispersity on the Conformation of Spherical Polymer Brushes. *ACS Macro Lett.* **2021**, *10*, 518–524.

(36) Ohno, K.; Morinaga, T.; Takeno, S.; Tsujii, Y.; Fukuda, T. Suspensions of silica particles grafted with concentrated polymer brush: Effects of graft chain length on brush layer thickness and colloidal crystallization. *Macromolecules* **2007**, *40*, 9143–9150.

(37) Wei, Y.; Xu, Y.; Faraone, A.; Hore, M. J. Local structure and relaxation dynamics in the brush of polymer-grafted silica nanoparticles. *ACS Macro Lett.* **2018**, *7*, 699–704.

(38) Layer, H.-S. O. O. Polymers at an Interface; A Simplified View PG de Gennes. *Simple Views Condens. Matter* **1998**, *8*, 260.

(39) Wijmans, C.; Zhulina, E. B. Polymer brushes at curved surfaces. *Macromolecules* **1993**, *26*, 7214–7224.

(40) Hansoge, N. K.; Huang, T.; Sinko, R.; Xia, W.; Chen, W.; Keten, S. Materials by design for stiff and tough hairy nanoparticle assemblies. *ACS Nano* **2018**, *12*, 7946–7958.

(41) Bobbili, S. V.; Milner, S. T. Chain tension reduces monomer friction in simulated polymer melts. *J. Rheol.* **2020**, *64*, 1373–1378.

(42) Bilchak, C. R.; Jhalaria, M.; Adhikari, S.; Midya, J.; Huang, Y.; Abbas, Z.; Nikoubashman, A.; Benicewicz, B. C.; Rubinstein, M.; Kumar, S. K. Understanding gas transport in polymer-grafted nanoparticle assemblies. *Macromolecules* **2022**, *55*, 3011–3019.

(43) Burgess, W. H.; Hopfenberg, H.; Stannett, V. Transport of noble gases in poly (methyl acrylate). *Journal of Macromolecular Science, Part B: Physics* **1971**, *5*, 23–40.

(44) Rohatgi, A. *Webplotdigitizer: Version 4.6*, 2022. <https://automeris.io/WebPlotDigitizer>.